Fuel Processing Technology 118 (2014) 228–234

Contents lists available at ScienceDirect

Fuel Processing Technology

journal homepage: www.elsevier.com/locate/fuproc

TGA–FTIR investigation of co-combustion characteristics of blends of hydrothermally carbonized oil palm biomass (EFB) and coal

Ganesh K. Parshetti, Augustine Quek, Raghu Betha, Rajasekhar Balasubramanian *

Minerals, Metals and Materials Technology Centre, National University of Singapore, EA Engineering Drive 1, Singapore 117576, Singapore
Department of Civil and Environmental Engineering, National University of Singapore, EA Engineering Drive 1, Singapore 117576, Singapore

ARTICLE INFO

Article history:
Received 1 May 2013
Received in revised form 20 September 2013
Accepted 29 September 2013
Available online 19 October 2013

Keywords:
Coal
EFB biomass
Hydrochar
Pollutant emissions
TGA–FTIR

ABSTRACT

Hydrothermally upgraded chars with improved density and friable characteristics were produced from oil-palm empty fruit bunch (EFB) at three temperatures (150, 250, and 350 °C—denoted as H-150, H-250 and H-350). These chars were co-combusted with low rank Indonesian coal and with hydrothermally upgraded coal (HT-coal). The composition of major gaseous pollutants released from the co-combustion process with specific reference to CO, CO_2, CH_4, NO, and SO_2 was studied in real-time using a thermogravimetric analyzer coupled with a Fourier transform infrared spectrometry. Combustion characteristic factor (*CCF*) was determined for a systematic analysis of the thermal decomposition process. In the co-combustion of hydrothermally treated biomass with coal and HT-coal, H-250 (50%)/HT-coal (50%) ($CCF = 4.1 \times 10^{-7}$) fuel blend showed the highest *CCF* values i.e. the most efficient co-combustion process. Further analysis of the emission profiles of gaseous pollutants revealed that the co-combustion of 50% H-350 with 50% HT-coal by mass produced the lowest levels of gaseous pollutant emissions. Overall, a systematic combustion carried out in this study showed that co-combustion of hydrothermally upgraded EFB biochar with coal and HT-coal leads to environmental benefits, specifically reduced emissions of toxic (CO), acidic (NO and SO_2) and greenhouse (CH_4 and CO_2) gases.

© 2013 Elsevier B.V. All rights reserved.

1. Introduction

Oil-palm empty fruit bunch (EFB), the primary solid waste of palm oil mill processing, is abundantly available in South-east Asia (Malaysia, Indonesia and Thailand). According to Yusoff [1], agriculture residues from oil palm industries consist of 13.5% mesocarp fiber, 5.5% palm kernel shell and 22% EFB. Malaysia has approximately 362 palm oil mills, processing about 82 million tons of fresh fruit bunch and producing an estimated 33 million tons of crop residue annually in the form of EFB, fiber and shell [2]. Lignocellulosic EFB (38.1–59.7 wt.% cellulose, 16.8–22.1 wt.% hemicelluloses, and 10.5–18.1 wt.% lignin) is potentially a low-cost material for production of energy densified carbonaceous products [3]. Direct co-combustion of EFB with coal is another way to generate heat or energy from this waste biomass [4,5]. During the co-firing, high carbon contents of the coal and the highly volatile nature of the biomass can compensate each other and may provide a better temperature profile for the combustion process than individual fuels do [6]. The cofiring of coal–biomass blends containing up to 20 wt.% biomass in utility pulverized fuel (PF) boilers has been successfully implemented in many countries [7]. Blends with 50 wt.% and 100 wt.% biomass have also been utilized [8]. Compared with the blends with 20 wt.% biomass content [8], the blends with 50 wt.% biomass showed better performance, with higher combustion efficiency and lower CO_2 emissions. Low-rank coal such as lignite and sub-bituminous coal is also frequently carbonized and upgraded by a hydrothermal treatment (HT) prior to its co-combustion with biomass for heat or power generation [9–12]. The upgraded coal by the HT process has lower moisture and oxygen contents compared to raw coal [9,12]. However direct cofiring systems are also more sensitive to variations in biomass or waste quality, moisture and heterogeneity [13–15]. Additionally, other problems limit the rate of secondary fuel use in place of the original fossil fuels. For example, ash deposition (fouling and slagging) and corrosion usually increase with the use of biomass replacing coal, which may shorten the lifespan of diverse devices such as boilers [16,17]. Direct cofiring systems include next technological solutions such as pretreatment of biomass by hydrothermal carbonization (HTC) [12,18–22]. HTC is a pressurized thermal conversion process, conducted at relatively low temperatures (150–350 °C). HTC accelerates biomass coalification by a factor of 10^6–10^9 under rather soft conditions, down to a scale of hours, and also makes it a considerable, technically-attractive alternative for the sequestration of carbon from biomass on large and ultra-large scales [23,24]. Moreover, the quality of the HTC coal as fuel as compared to the raw material is improved due to its higher calorific value, less moisture and its handling and storage properties [24]. In addition, inorganic substances are leached into the process water, which reduces the ash content of the product [25].

---

* Corresponding author at: Department of Civil and Environmental Engineering, National University of Singapore, EA Engineering Drive 1, Singapore 117576, Singapore. Tel.: +65 6516 5135; fax: +65 6872 5483.
E-mail address: ceerbala@nus.edu.sg (R. Balasubramanian).

0378-3820/$ – see front matter © 2013 Elsevier B.V. All rights reserved.
http://dx.doi.org/10.1016/j.fuproc.2013.09.010

Most of the previous investigations on coal/biomass co-combustion have focused on mass loss rate as a function of various operational parameters such as heating rate and sample size [4,5,26–30]. However, the real time analysis of the production and release of gaseous pollutants during the course of co-combustion of hydrothermally treated coal/biomass has rarely been studied. In order to predict the behavior of hydrothermally prepared char during co-combustion with natural coal and hydrothermally upgraded coal, it is very important to understand its emission characteristics from the environmental point of view. The distinct feature of our study is the combustion behavior and gaseous emission analysis of blends of hydrothermally treated EFB biomass and coal. Gaseous pollutants that are generally formed during thermal decomposition of organics and bio-polymers such as biomass are carbon dioxide (CO_2), carbon monoxide (CO), methane (CH_4), ethane (C_2H_4), ammonia (NH_3), hydrocyanic acid (HCN), sulfur dioxide (SO_2) and carbonyl sulfide (COS) [31–33]. Fang et al. [34] found that the following gaseous products were emitted from thermal decomposition of different biomass types (merbau, cotton straw, birch)—CO_2, CO, H_2O, CH_4, acetic acid (CH_3COOH) and methanol (CH_3OH). Information on the type, quantity and time of release of gaseous products is essential to get a complete understanding of the fundamentals and mechanisms involved in the thermal decomposition process and also to formulate effective pollution control strategies. The use of thermogravimetric analysis (TGA) in conjunction with Fourier transform infrared spectrometry (FTIR) is an effective approach to obtain the composition of evolved gases on the basis of their specific absorbance as biomass is thermally decomposed [7,32,33]. We have recently reported EFB conversion to solid carbonaceous materials (hydrochars) using hydrothermal carbonization (HTC) and its co-combustion with coal for energy production [18].

In the present work, we have studied the emission behavior of EFB biomass and its hydrochar with coal as well as with hydrothermally treated coal by the TGA–FTIR method. This work aimed at conducting a systematic examination of the emission characteristics of gaseous pollutants (CO, CO_2, CH_4, NO and SO_2) using a TGA-FTIR system during co-combustion of EFB biomass and its hydrochars produced at different hydrothermal temperatures with low rank Indonesian coal and hydrothermally upgraded coal (HT-coal) blends. The combustion characteristic factor (S) as well as emissions of gaseous pollutants from solid fuels and their blends were evaluated.

2. Materials and methods

2.1. Materials

In this study, EFB was obtained from an oil processing company in Malaysia. EFB is the lignocellulosic material remaining as a by-product of the industrial palm oil process after removal of the nuts. To promote homogeneous mixing of EFB, and to facilitate its effective conversion to hydrochar during HTC treatment, the EFB was processed into fine pieces (1–6 mm) using a grinder, then air-dried and stored in a sealed container until use. Low rank Indonesian coal was obtained from a coal mining company in Jakarta, Indonesia. Coal was manually chopped into small pieces to promote homogeneous mixing and facilitate their effective up-grading during the HTC treatment.

2.2. Hydrothermal carbonization: apparatus and procedure

HTC of EFB was carried out in a 500 mL Parr stirred pressure batch reactor (model 4575). In a typical run, 25 g of previously dried EFB was dispersed in 250 mL of de-ionized water contained in the reactor. Experiments were conducted at different temperatures (150, 250 and 350 °C) with a constant reaction time of 20 min. For coal upgrading at 250 °C (20 min), 25 g of coal was dispersed in 250 mL of de-ionized water in the reactor. The reactor was sealed and heated to the desired reaction temperature in an electric furnace. After the desired residence time, the reactor was rapidly cooled to quench the reaction. Residence time is defined as the time the reactor is held and operated at the desired reaction temperature, excluding preheating and cooling time. After the reactor cooled down to the room temperature, it was opened to collect the solid carbonaceous products. The solid product (hydrochar) was recovered by filtration, washed with deionized water and dried in air. The char product was weighed independently and stored in a sealed container until analysis.

2.3. Characterization of hydrochar

The 5E-MAG6600 automatic proximate analyzer was used to determine the weight percentages (wt.%) of moisture, volatile matter, fixed carbon and ash in EFB, coal and HT-coal. An elemental analyzer (vario MACRO cube, ELEMENTAR, Germany) was used to carry out ultimate analyses to determine the weight percentages of chemical elements (carbon, hydrogen, nitrogen, oxygen and sulfur) in the EFB, coal and HT-coal. In the present study, combustion of all the samples were performed in the furnace of the Perkin Elmer TGA7 system operated at a gas flow (mixture of N_2 (70%) and O_2 (30%)), rate of 100 mL min^{-1} while heating from 25 to 900 °C at the rate of 20 °C min^{-1}. All fuel samples were ground to micron-sized particles and these particles were placed upon a sieve that passed particles of less than 150 μm (micron). Thus, the particle size of the fuels was approximately 150 μm for TGA analysis. The weight loss (TG) and the rate of weight loss (DTG) were analyzed to find the key combustion parameters. The ignition temperature and burnout temperatures were determined using the TG-DTG (the first derivative of TG curve) method based on previous publications in the literature [19,20]. In brief, the ignition temperature (T_o) was determined based on the temperature at which the DTG had its peak value and the corresponding slope to the intersection with respect to the TG profile. The burnout temperature (T_f) was detected based on the mass stabilization. The gas products from the combustion of samples in TGA were determined using a coupled, on-line Fourier transform infrared spectrometer (Perkin-Elmer FTIR Spectrum 2000). While other conditions were kept the same as those used in TGA, the sample was controlled at ~20 mg to provide enough gas for analysis. To minimize the secondary reaction, the gaseous products released from thermogravimetric balance were swept immediately to a gas cell, followed by detection using the FTIR spectrometer. The transfer line and the head of the TG balance were heated at a constant temperature of 200 °C, to avoid the condensation of volatile decomposition products. The IR was used in a scanning range of 4000–400 cm^{-1}, in terms of wave number. The resolution and sensitivity were set at 4 cm^{-1} and 1, respectively. FTIR spectra of the gaseous products were collected continuously with the baseline corrected.

3. Results and discussion

3.1. Fuel characteristics

The proximate analysis, ultimate analysis and calorific values of EFB, coal and HT-coal are shown in Table 1. As can be seen from the table, the volatile mater in the EFB biomass (82.2% ± 4.3) was almost two times higher than that in coal (56.4% ± 3.4) and HT-coal (48.0% ± 2.9). On the other hand, coal and HT-coal had higher fixed carbon and higher moisture contents in this study. Among the EFB, coal and HT-coal fuels used in this study, coal had the highest ash content (3.2% ± 0.2). The results of ultimate analyses are also given in Table 1. The ultimate analyses revealed the high contents of carbon in both coal and HT-coal (i.e., 45.4 ± 2.7 and 55.2 ± 3.32 wt.%, respectively), suggesting a high proportion of organic carbon. Also it can be seen from Table 1, that the coal (1.22% ± 0.07) and HT-coal (1.25% ± 0.07) has higher sulfur content than that of the EFB biomass (0.34% ± 0.01). The higher heating value (HHVs) [35] of HT-coal (22.30 ± 1.35 MJ kg^{-1}) was relatively higher than that of coal (20.71 ± 1.10 MJ kg^{-1}) and EFB biomass

Table 1
Physical–chemical analysis and calorific values of the EFB, coal and HT-coal.

Property	EFB	Coal	HT-coal
Elemental analysis (%) (daf)[a]			
Carbon	48.30	47.06	55.18
Hydrogen	6.66	5.86	5.28
Nitrogen	1.00	1.48	1.73
Sulfur	0.34	1.22	1.25
Oxygen (by difference)	43.70	44.38	36.56
Atomic ratio			
O/C	0.67	0.84	0.49
H/C	1.65	1.55	1.15
Proximate analysis (%)			
Moisture	4.29	10.69	9.08
Volatiles	82.21	52.45	47.08
Ash	3.09	3.22	2.10
Fixed carbon	10.41	33.64	41.74
HHV (MJ kg^{-1})[b]	17.93	20.71	22.30

[a] Dry ash-free.
[b] HHV (high heating value) = 0.196 (FC) + 14.119 [45].

(17.93 ± 0.91 MJ kg^{-1}). The HT-coal produced had the calorific value of 22.30 ± 1.35 MJ kg^{-1} which is higher than that of the coal (20.71 ± 1.10 MJ kg^{-1}), suggesting that the hydrothermal treatment results in further densification of coal, which can be attributed to a decrease in the ratios of both the O/C (0.51 ± 0.03) and H/C (1.15 ± 0.06) when coal was subjected to the pre-treatment. At higher HTC operating temperatures, the dehydration process became obvious. A decrease in the O/C ratio suggests that decarboxylation also occurs during the HTC of coal [18]. To determine the interactive effects of EFB biomass and its hydrochars (H-150, H-250 and H-350) during their co-combustion with coal and HT-coal, a blending ratio of 50% was used. The combustion properties determined from the TG/DTG analysis are presented in Table 2. A parameter called the combustion characteristic factor (*CCF*) [7] was used as a criterion for fuel combustion performance, and is defined below as:

$$s = \frac{\left(\frac{dw}{dt}\right)_{max} \left(\frac{dw}{dt}\right)_{mean}}{T_{i^2} T_h} \tag{1}$$

where $(dw/dt)_{max}$ is the maximum burning velocity (% min^{-1}); $(dw/dt)_{mean}$ is the average burning velocity (% min^{-1}); T_i is the ignition temperature (K); and T_h is the burnout temperature (K). This factor, which includes the ease of ignition, the firing velocity and the burnout temperature, is a comprehensive combustion parameter. *CCF* was used to compare the combustion performance of different fuels and their blends, and the *CCF* values are listed in Table 2. With the exception of coal, EFB (50%)/coal (50%), HT-350 (50%)/coal (50%) blends, the values are close to or greater than 2 for all other fuels and blends, indicating their good general combustion performance [7]. The *CCF* values for the hydrochar/HT-coal blends were found to be higher than the values of the hydrochar/coal blends. This observation suggests that the EFB hydrochar has potential to improve the combustion performance of HT-coal while used in the form of pellets after the blending. Addition of hydrothermally carbonized oil palm biomass (EFB) has shown better burning characteristics because of its improved fuel qualities compared to the raw EFB biomass, such as decreased volatile matter/(volatile matter + fixed carbon) ratio and increased carbon content [18]. Further, the energy density of EFB hydrochar increased with increasing hydrothermal temperature, with higher heating values being close to those of natural coal. Also, the addition of hydrothermally carbonized oil palm biomass (EFB) lowers the activation energy required during co-combustion with coal [18]. Fuels blends with high *CCF* values, for example, HT-250 (50%) + coal (50%) ($CCF = 3.02 \times 10^{-7}$) and HT-250 (50%) + HT-coal (50%) ($CCF = 4.14 \times 10^{-7}$), are promising candidates that can be used as solid fuels for energy generation.

Table 2
Combustion characteristic factor (S) from the TG/DTG analysis for fuels.

Combust-properties	$(dm/dt)_{max}$ (%min^{-1})	$(dm/dt)_{mean}$ (%min^{-1})	T_o (°C)[a]	T_f (°C)[b]	$S \times 10^{-7}$
EFB	29.12	1.88	220	662	2.40
Coal	24.15	2.14	340	438	1.93
HT-coal	29.51	2.18	330	430	2.52
EFB (50%) + coal (50%)	30.90	1.89	328	610	1.83
EFB (50%) + HT-coal (50%)	38.68	2.18	318	600	2.77
HT-150 (50%) + coal (50%)	35.07	2.45	345	640	2.47
HT-150 (50%) + HT-coal (50%)	43.97	2.48	350	660	3.00
HT-250 (50%) + coal (50%)	46.32	2.47	360	672	3.02
HT-250 (50%) + HT-coal (50%)	63.42	2.42	355	667	4.14
HT-350 (50%) + coal (50%)	30.82	1.87	340	655	1.65
HT-350 (50%) + HT-coal (50%)	46.12	2.46	365	660	2.98

[a] T_o = ignition temperature.
[b] T_f = burnout temperature.

3.2. TGA–FTIR analysis of gas products

TGA has been demonstrated to be a very valuable technique for studying the combustion of a wide range of solid samples [7,33,36,37]. When FTIR is used as a complementary technique with TGA, it will provide insightful information on the composition of gaseous products as they evolve from the combustion of solid fuels. We therefore used TGA coupled with FTIR in this study to investigate the combustion behavior of all solid fuels and their blends and measure the emission of major gaseous pollutants of environmental concern at the heating rate of 20 °C min^{-1}. Fig. 1 shows a schematic diagram of the TGA–FTIR system used in the current study. During the combustion cracking process, the gases released in the TGA were swept immediately to a gas cell, followed by FTIR analysis. A typical three-dimensional plot of the spectra obtained from the gas volatized during the thermal decomposition of EFB biomass in the temperature range of 25–900 °C is shown in Fig. 2a; this temperature refers to the operating temperature of the TGA. The volatiles identified with TGA–FTIR analysis in the current study are CH_4 (2978 cm^{-1}), CO (2119 cm^{-1}), CO_2 (2360 & 670 cm^{-1}), NO (1762 cm^{-1}) and SO_2 (1342 cm^{-1}) (as shown in Fig. 2b) for individual fuels based on the spectral information available from the literature [7,33,36,37]. According to the TGA–FTIR study, the evolution of gaseous products increases with the combustion temperature, reaching their maximum values between 220 and 500 °C. Generally, the peak at 3580 cm^{-1} is assigned to the symmetric and asymmetric stretching vibrations of H_2O molecules while those in the range of 3700–3900 cm^{-1} may be associated with rota-vibrational bands of water vapor [38]. As the combustion temperature increases between 220 and 500 °C, the release of CO_2, CO, CH_4, NO and SO_2 rises significantly (Figs. 3–7). The detection of both CO_2 and CO in this temperature range suggests that the decarboxylation (formation of CO & CO_2) reactions are simultaneously favored in this stage of the combustion [38]. At the higher temperature range from 600 °C to 900 °C, the release of pollutant gases was almost negligible, indicating the completion of combustion (Figs. 3–7) [39,40].

3.2.1. CO_2 emission patterns

Fig. 3 shows the emission of CO_2 from the combustion of EFB, coal and HT-coal and their hydrochar blends at different combustion temperatures. The CO_2 emission profiles for EFB, coal, coal/EFB and coal/hydrochar blends showed two peaks, one in the range of 220 to 420 °C and the other in the range of 420 to 550 °C. However, the first

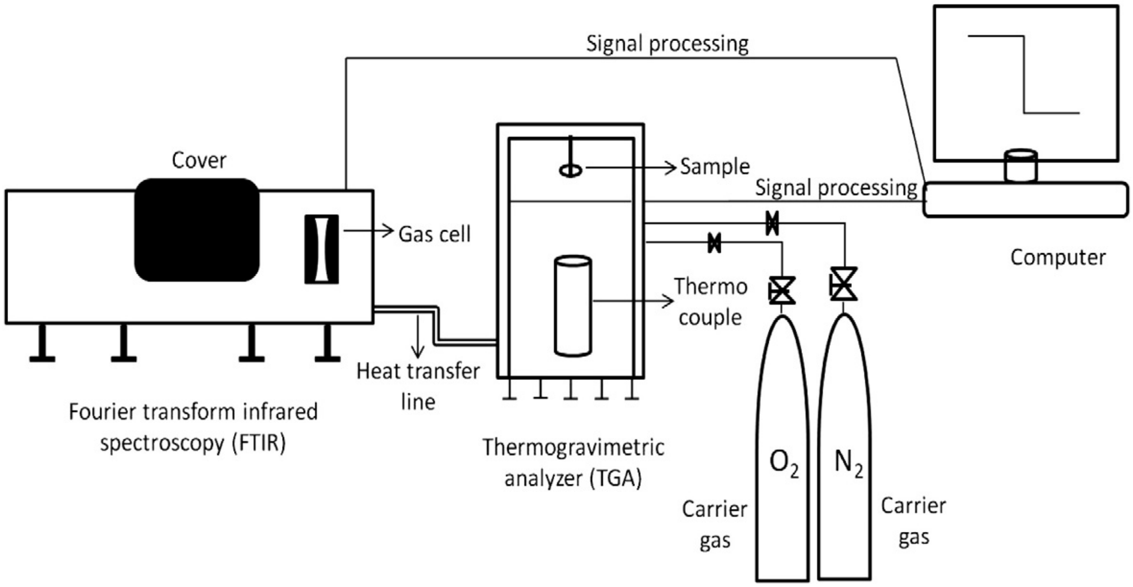

Fig. 1. Schematic diagram of the TGA–FTIR system.

peak reflecting a strong emission of CO_2 was more prominent than the second peak. This observation suggests that the CO_2 emission was relatively higher during the combustion of volatile matters which occurred in the temperature range of 220 to 420 °C. However, the level of CO_2 emission decreased significantly when the combustion temperature increased to the range of 420 to 550 °C at which the char burning appears to have been started. For the HT-coal, HT-coal/EFB and HT-coal/hydrochar blends, the emission profile of CO_2 had only one peak, suggesting that the major combustion process took place during the initial burning period i.e. 220 to 420 °C. Fig. 3 also shows that the CO_2 released had its maximum value for coal based on the absorbance value, which continued to increase beyond the temperature region at which the thermal decomposition occurred (i.e. >550 °C). Possible reasons for the increased emissions of CO_2 include thermal cracking of solid residues left in the fuels, oxidation of the carbonized char, and high temperature thermal decomposition [40–42]. The magnitude of the CO_2 emission was generally 10 to 30 times higher than that of other detected gases (CO, CH_4, SO_2 and NO as presented in Figs. 4 to 7) in the present study. For the HT-coal and HT-coal/hydrochar blends, the CO_2 emission peak shifted to lower temperatures than what was observed for coal and coal/hydrochar blends. The total CO_2 emission was completely influenced by the contents of fuel in the blends. This was confirmed by the integral areas under the emission curves which are 14.015 for

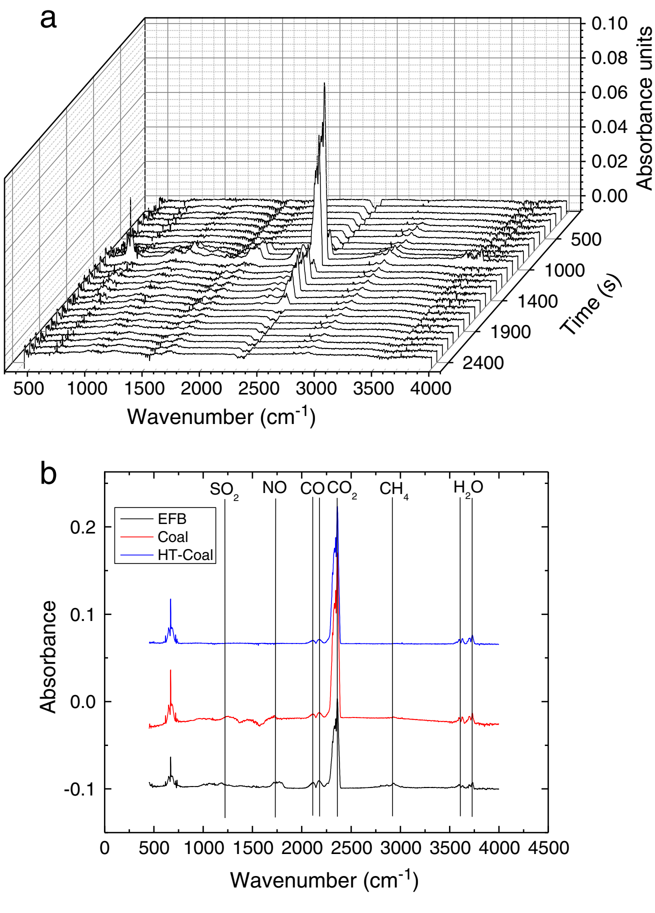

Fig. 2. Three-dimensional (3D) FTIR spectral plot of the gases emitted from the combustion of (a) EFB biomass and (b) FTIR spectral plot of the gases produced from the combustion of EFB, coal and HT-coal at a heating rate of 20 °C/min in TGA–FTIR.

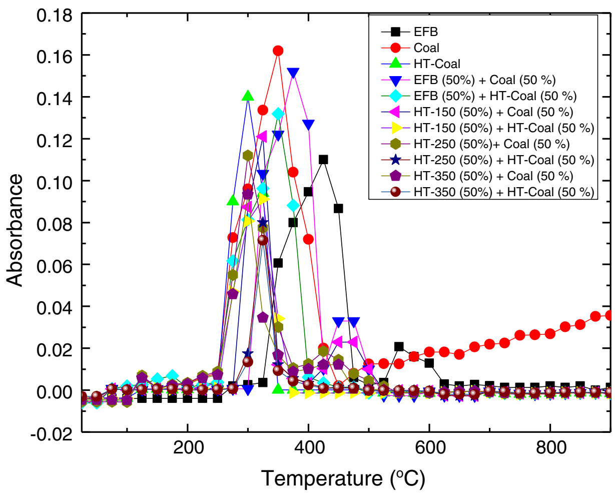

Fig. 3. Evolution of CO_2 against the sample bed temperature for the different blends of fuels at a heating rate of 20 °C/min in TGA–FTIR.

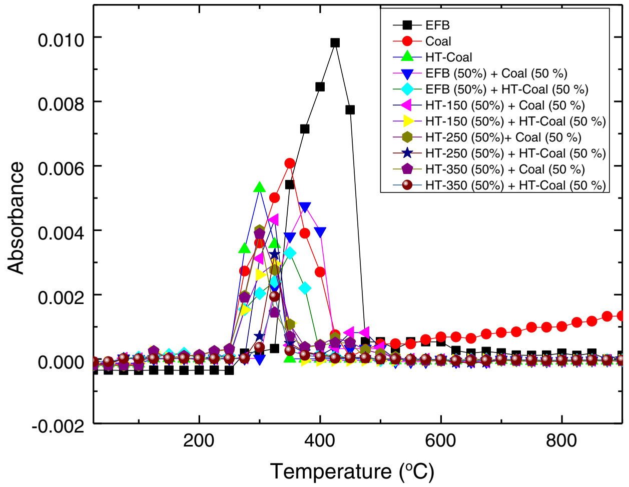

Fig. 4. Evolution of CO against the sample bed temperature for the different blends of fuels at a heating rate of 20 °C/min in TGA–FTIR.

EFB (50%)/coal (50%), 11.708 for EFB (50%)/HT-coal (50%), 6.814 for HT-150 (50%)/coal (50%), 5.532 for HT-150 (50%)/HT-coal (50%), 8.409 for HT-250 (50%)/coal (50%), 2.469 for HT-250 (50%)/HT-coal (50%), 5.689 for HT-350 (50%)/coal (50%) and 2.149 for HT-350 (50%)/HT-coal (50%) (Table 3). These results prove that the blending of EFB hydrochar with coal and HT-coal can reduce CO_2 emissions significantly. The hydrothermal treatment changes the properties of hydrochar products the same way as the natural coalification process occurs. The solid product EFB hydrochar formed from hydrothermally treated EFB biomass is largely formed by recondensation reactions owing to the evolution of H_2O and CO_2 in the dehydration and decarboxylation reactions, which lower the O/C ratios than the initial biomass product [18]. The atomic H/C and O/C ratios decreased while increasing the hydrothermal reaction temperature. Most of the original feedstock was lost in the form of gaseous (i.e., H_2, CO and CO_2) and liquid by-products. In addition, under hydrothermal treatment temperatures, most of the original carbon stays bound to the final structure of the hydrochar. Carbon structures produced by this route are, therefore, most CO_2-efficient and help in reduce CO_2 emissions when used in co-combustion processes. Furthermore, the blending of untreated EFB biomass itself with coal and HT-coal could also help in CO_2 reduction, but the emission of

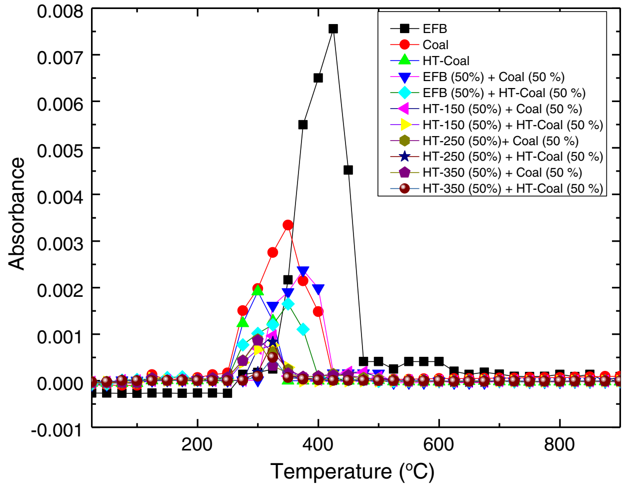

Fig. 5. Evolution of CH_4 against the sample bed temperature for the different blends of fuels at a heating rate of 20 °C/min in TGA–FTIR.

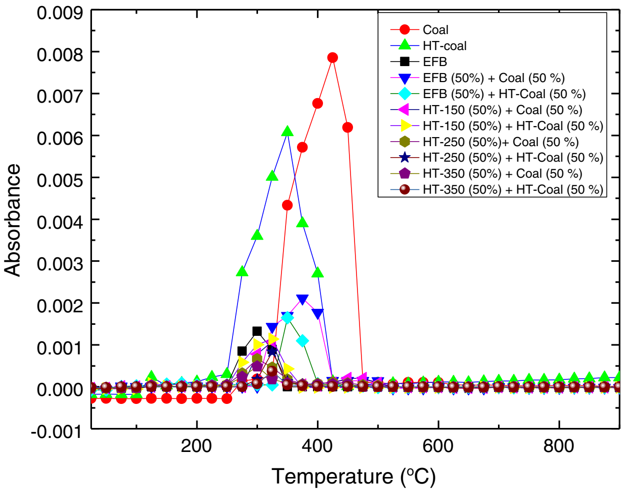

Fig. 6. Evolution of SO_2 against the sample bed temperature for the different blends of fuels at a heating rate of 20 °C/min in TGA–FTIR.

other gases should also be considered as discussed in the sections below.

3.2.2. CO emission patterns

The CO emission profiles for the fuel samples are shown as a function of combustion temperature in Fig. 4. All profiles showed a single peak except that of EFB biomass. The highest CO emission occurred at about 425 °C for the EFB biomass. In addition, a minor secondary peak appeared in the range of 520 to 620 °C. The initial stage of CO release was probably caused by the decarboxylation reaction of alkyl side-chains containing the carbonyl functional groups (—CHO) of lignocellulosic EFB biomass, while the increase of CO at the high temperatures was probably due to secondary reactions [39,40,43]. For coal beyond 500 °C, the CO emission increased slowly with temperature rising up to 900 °C as was seen for CO_2. The increase in CO beyond 550 °C might be due to the thermal cracking of evolved tar downstream of the TGA sample holder [32]. Tar is a mixture of various unknown compounds that are present in TGA–FTIR system as fine aerosol or condensable material [44]. The CO emission of all fuel blends started around 230 °C and presented differences in the peak position/height due to differences in the relative contents of the main constituents. The EFB/coal and EFB/HT-coal blend decomposed at higher temperatures with a peak around

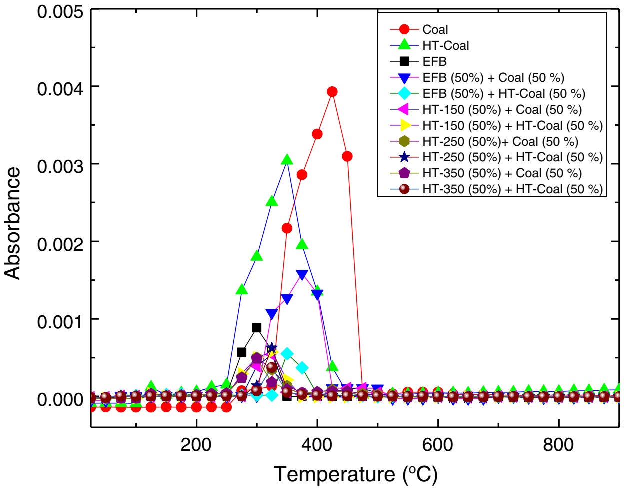

Fig. 7. Evolution of NO against the sample bed temperature for the different blends of fuels at a heating rate of 20 °C/min in TGA–FTIR.

Table 3
Yields of CO_2, CO, CH_4, NO and SO_2 species from combustion of various fuels.

Property	EFB	Coal	HT-Coal	EFB (50%) + Coal (50%)	EFB (50%) + HT-Coal (50%)	HT-150 (50%) + Coal (50%)	HT-150 (50%) + HT-Coal (50%)	HT-250 (50%) + Coal (50%)	HT-250 (50%) + HT-Coal (50%)	HT-350 (50%) + Coal (50%)	HT-350 (50%) + HT-Coal (50%)
CO_2 integral value	12.101	26.161	7.482	14.015	11.708	6.814	5.532	8.409	2.469	5.689	2.149
CO integral value	1.018	0.981	0.283	0.377	0.292	0.243	0.180	0.300	0.100	0.237	0.058
CH_4 integral value	0.697	0.361	0.102	0.201	0.146	0.054	0.046	0.066	0.025	0.052	0.014
SO_2 integral value	0.070	0.743	0.671	0.178	0.076	0.060	0.069	0.050	0.025	0.026	0.010
NO integral value	0.047	0.371	0.337	0.134	0.025	0.030	0.034	0.037	0.019	0.029	0.011

375 and 350 °C, respectively compared to other blends. Individual CO emission peaks for hydrochar/coal and hydrochar/HT-coal blends were very close to each other compared to EFB/coal and EFB/HT-coal blends. The integral areas under the emission curves are 0.377 for EFB (50%)/coal (50%), 0.292for EFB (50%)/HT-coal (50%), 0.243 for HT-150 (50%)/coal (50%), 0.180 for HT-150 (50%)/HT-coal (50%), 0.300 for HT-250 (50%)/coal (50%), 0.100 for HT-250 (50%)/HT-coal (50%), 0.237 for HT-350 (50%)/coal (50%) and 0.058 for HT-350 (50%)/HT-coal (50%) (Table 3). These results reveal that the blending of EFB hydrochar with coal and HT-coal decreases CO emissions considerably.

3.2.3. CH_4 emission patterns

The CH_4 emission profiles for all the fuel samples and blends are shown as a function of temperature in Fig. 5. All profiles show dispersed peaks in the temperature range of 230 to 600 °C when the volatile matter and char were burnt rapidly. The EFB biomass showed two peaks one at 425 and the other at 575 °C, suggesting two burning processes involving volatile materials and fixed carbon. The release of CH_4 in the fixed carbon stage was much lower than that in the volatile material stage. A temperature gap of more than 150 °C was observed for these two stages. The emission of CH_4 at later stage (575 °C) was probably due to the release of methoxyl groups, resulting mainly from lignin decomposition [40,43]. Except for the EFB biomass, the CH_4 emission beyond 450 °C was almost negligible with the combustion temperature rising up to 900 °C. There were also few differences in the CH_4 emission profiles for different blends of solid fuels. For EFB (50%)/coal (50%), and EFB (50%)/HT-coal (50%), the CH_4 emission peaks were mainly observed at the fixed carbon burning stage between 350 and 380 °C, whereas for HT-150 (50%)/coal (50%), HT-150 (50%)/HT-coal (50%), HT-250 (50%)/coal (50%), HT-250 (50%)/HT-coal (50%), HT-350 (50%)/coal (50%) and HT-350 (50%)/HT-coal (50%) the CH_4 emission peaks were mainly observed at the volatile burning stage between 275 and 340 °C. For the hydrochar blends with coal such as HT-150 (50%)/HT-coal (50%), HT-250 (50%)/HT-coal (50%) and HT-350 (50%)/HT-coal (50%), the peak CH_4 emission level was much lower than that of the other blends. It appeared that the HT-350 (50%)/HT-coal (50%) blend produced the lowest total emission in CH_4. This was confirmed by integrating the area under emission curves for each of the samples. The integral areas under the emission curves are 0.201 for EFB (50%)/coal (50%), 0.146for EFB (50%)/HT-coal (50%), 0.054 for HT-150 (50%)/coal (50%), 0.046 for HT-150 (50%)/HT-coal (50%), 0.066 for HT-250 (50%)/coal (50%), 0.025 for HT-250 (50%)/HT-coal (50%), 0.052 for HT-350 (50%)/coal (50%) and 0.014 for HT-350 (50%)/HT-coal (50%) (Table 3).

3.2.4. SO_2 emission pattern

Fig. 6 shows the existence of a single peak for SO_2 for all fuel samples and blends. The ultimate analysis showed that the amount of S in EFB biomass was less than that in the coal and HT-coal, therefore, the extent of release and the intensity for SO_2 in the coal and HT-coal were much higher than that for EFB. The highest SO_2 emission occurred at about 420 °C and 355 °C for coal and HT-coal, respectively. The SO_2 emission levels in the peak were reduced with addition of the EFB hydrochar in the blends; such reductions are expected because of a lower overall fuel-bound S content and a displacement of sulfur in the fuel blend [45]. The features of the SO_2 peak were more strongly influenced by the fuel compositions of the blends. Among all blends, the SO_2 emission magnitude was higher for the two blends viz. EFB (50%)/coal (50%) and EFB (50%)/HT-coal (50%) and the SO_2 peak also shifted slightly towards the lower temperature with the HT-coal contents. The blend which produced lower SO_2 during combustion was HT-350 (50%)/HT-coal (50%). This was confirmed from the integral areas (Table 3) of the SO_2 emission curves, which are 0.671 for HT-coal, 0.178 for EFB (50%)/coal (50%), 0.076 for EFB (50%)/HT-coal (50%), 0.060 for HT-150 (50%)/coal (50%), 0.069 for HT-150 (50%)/HT-coal (50%), 0.050 for HT-250 (50%)/coal (50%), 0.025 for HT-250 (50%)/HT-coal (50%), 0.026 for HT-350 (50%)/coal (50%) and 0.010 for HT-350 (50%)/HT-coal (50%).

3.2.5. NO emission pattern

Fig. 7 showed the NO emission profiles for different fuels. Coal used in the current research has low nitrogen contents. Consequently, the NO emission level was also low and was similar to SO_2 emissions in terms of its magnitude. It can be seen clearly from Fig. 7 that all NO emission profiles show a single peak unlike the emission patterns observed for CO_2, CO and CH_4. The NO emission peak appeared at about 426 °C for the coal which showed a maximum emission (Integral area: 0.371). Further, HT-coal (integral area: 0.337) and EFB(50%)/coal(50%) blends (integral area: 0.134) also showed comparatively higher emissions of NO with peaks at 352 and 375 °C, respectively. As reported in the literature [46,47], high-temperature combustion produces more NO, named "thermal NOx" similar to the process in grate combustion. However, for most of the fuels and blends studied here, a very low amount of NO was released in the high-temperature range. The high volatile contents of biomass derived hydrochar can effectively establish a fuel-rich zone early in the flame that can reduce NO_x emissions. Adding hydrochar can also reduce flame temperatures, leading to lower levels of thermal NO_x [45]. The degree of the NO peak decreased with the addition of various hydrochar contents in the blends. The solid sample which produced lower NO during combustion and resisted the thermal formation at high temperature is HT-350 (50%)/HT-coal (50%). This is confirmed in the integral areas of the NO emission curves, which are 0.337 for HT-coal, 0.025 for EFB (50%)/HT-coal (50%), 0.030 for HT-150 (50%)/coal (50%), 0.034 for HT-150 (50%)/HT-coal (50%), 0.037 for HT-250 (50%)/coal (50%), 0.019 for HT-250 (50%)/HT-coal (50%), 0.029 for HT-350 (50%)/coal (50%) and 0.011 for HT-350 (50%)/HT-coal (50%) (Table 3).

4. Conclusions

The emission characteristics of gaseous pollutants released from the combustion of untreated EFB biomass and its hydrochars with coal and HT-coal were investigated by TGA–FTIR. The combustion of solid carbonaceous fuels in the temperature range of 220 °C to 500 °C led to a maximum release of gaseous pollutants such as CO_2, CO, CH_4, NO and SO_2 for all fuels and their blends investigated in this study. The key combustion parameter, *CCF*, for most of the fuels and/or their blends was greater than 2, indicating good combustion performance. The combustion behavior of fuels and their blends show that the burning process was better in blends such as HT-250 (50%) + coal (50%) and HT-250 (50%) + HT-coal (50%) where the rate of weight loss was at its maximum (*Rmax*) and the highest CCF value was also achieved, but the emission of gaseous pollutants (CO_2, CO, CH_4, NO and SO_2) was not at its minimum level. On the other hand for blends HT-350 (50%) + coal (50%) and HT-350 (50%) + HT-coal (50%) under similar conditions, the lowest amounts of gaseous pollutants (CO_2, CO, CH_4, NO and SO_2) were emitted but *Rmax* and CCF decreased. Thus for the experimental combustion and pollutant emission profiles of hydrochar/coal and hydrochar/HT-coal blend samples, some deviations were observed from the expected trends in terms of their *Rmax*, CCF values and emission characteristics. These deviations are indicative of synergistic interactions taking place between the fuels during co-combustion of EFB hydrochars and coal/HT-coal.

Overall, this study revealed that the addition of EFB hydrochars to coal and HT-coal resulted in a significant reduction in gaseous pollutant emissions along with good burning performance for some blends. Thus, co-combustion of hydrothermally upgraded waste biomass with coal or upgraded coal is an attractive option to consider in existing power plants for energy generation because of the major environmental benefits such as reduction in the emission of greenhouse gases (CO_2 and CH_4), acidic gases (SO_2 and NO) and toxic gas (CO). In addition, particulate emissions should also be investigated which is currently in progress in our laboratory.

Acknowledgments

The authors are thankful to the Singapore Economic Development Board (EDB) and the Minerals, Metals and Materials Technology Centre (M3TC), National University of Singapore for the financial support extended to this project.

References

[1] S. Yusoff, Renewable energy from palm oil — innovation on effective utilization of waste, Journal of Cleaner Production 14 (2006) 87–93.
[2] C.S. Goh, K.T. Tan, K.T. Lee, S. Bhatia, Bio-ethanol from lignocellulose: status, perspectives and challenges in Malaysia, Bioresource Technology 101 (2010) 4834–4841.
[3] N. Abdullah, H. Gerhauser, Bio-oil derived from empty fruit bunches, Fuel 87 (2008) 2606–2613.
[4] S.S. Idris, N.A. Rahman, K. Ismail, A.B. Alias, Z.A. Rashid, M.J. Aris, Investigation on thermochemical behaviour of low rank Malaysian coal, oil palm biomass and their blends during pyrolysis via thermogravimetric analysis (TGA), Bioresource Technology 101 (2010) 4584–4592.
[5] S.S. Idris, N.A. Rahman, K. Ismail, Combustion characteristics of Malaysian oil palm biomass, sub-bituminous coal and their respective blends via thermogravimetric analysis (TGA), Bioresource Technology 123 (2012) 581–591.
[6] S. De, M. Assadi, Impact of cofiring biomass with coal in power plants — a techno-economic assessment, Biomass and Bioenergy 33 (2009) 283–293.
[7] C.P. Wang, Y.J. Wu, Q. Liu, H.R. Yang, F.Y. Wang, Analysis of the behaviour of pollutant gas emissions during wheat straw/coal cofiring by TG–FTIR, Fuel Processing Technology 92 (2011) 1037–1041.
[8] D.R. McIlveen-Wright, Y. Huang, S. Rezvani, Y. Wang, A technical and environmental analysis of co-combustion of coal and biomass in fluidised bed technologies, Fuel 86 (2007) 2032–2042.
[9] H. Katalambula, R. Gupta, Low-grade coals: a review of some prospective upgrading technologies, Energy & Fuels 23 (2009) 3392–3405.
[10] M. Morimoto, H. Nakagawa, K. Miura, Low rank coal upgrading in a blow of hot water, Energy & Fuels 23 (2009) 4533–4539.
[11] A.T. Mursito, T. Hirajima, K. Sasaki, Upgrading and dewatering of raw tropical peat by hydrothermal treatment, Fuel 89 (2010) 635–641.
[12] M. Nonaka, T. Hirajima, K. Sasaki, Upgrading of low rank coal and woody biomass mixture by hydrothermal treatment, Fuel 90 (2011) 2578–2584.
[13] C. Yin, L.A. Rosendahl, S.K. Kaer, Grate-firing of biomass for heat and power production, Progress in Energy and Combustion Science 34 (2008) 725–754.
[14] X.G. Xu, S.Q. Li, G.D. Li, Q. Yao, Effect of co-firing straw with two coals on the ash deposition behavior in a down-fired pulverized coal combustor, Energy & Fuels 24 (2010) 241–249.
[15] Y.Y. Shao, C.B. Xu, J. Zhu, F. Preto, J.S. Wang, H.N. Li, C. Badour, Ash deposition in co-firing three-fuel blends consisting of woody biomass, peat, and lignite in a pilot-scale fluidized-bed reactor, Energy & Fuels 25 (2011) 2841–2849.
[16] F. Wigley, J. Williamson, A. Malmgren, G. Riley, Ash deposition at higher levels of coal replacement by biomass, Fuel Processing Technology 88 (2007) 1148–1154.
[17] Z. Gogebakan, Y. Gogebakan, N. Selcuk, E. Seliuk, Investigation of ash deposition in a pilot-scale fluidized bed combustor co-firing biomass with lignite, Bioresource Technology 100 (2009) 1033–1036.
[18] G.K. Parshetti, S. Kent Hoekman, R. Balasubramanian, Chemical, structural and combustion characteristics of carbonaceous products obtained by hydrothermal carbonization of palm empty fruit bunches, Bioresource Technology 135 (2013) 683–689.
[19] M. Muthuraman, T. Namioka, K. Yoshikawa, Characteristics of co-combustion and kinetic study on hydrothermally treated municipal solid waste with different rank coals: a thermogravimetric analysis, Applied Energy 87 (2010) 141–148.
[20] Z.G. Liu, A. Quek, S.K. Hoekman, M.P. Srinivasan, R. Balasubramanian, Thermogravimetric investigation of hydrochar-lignite co-combustion, Bioresource Technology 123 (2012) 646–652.
[21] M. Muthuraman, T. Namioka, K. Yoshikawa, A comparison of co-combustion characteristics of coal with wood and hydrothermally treated municipal solid waste, Bioresource Technology 101 (2010) 2477–2482.
[22] Y. Jin, L. Lu, X. Ma, H. Liu, Y. Chi, K. Yoshikawa, Effects of blending hydrothermally treated municipal solid waste with coal on co-combustion characteristics in a lab-scale fluidized bed reactor, Applied Energy 102 (2013) 563–570.
[23] M.M. Titirici, A. Thomas, M. Antonietti, Back in the black: hydrothermal carbonization of plant material as an efficient chemical process to treat the CO_2 problem? New Journal of Chemistry 31 (2007) 787–789.
[24] M.M. Titirici, R.J. White, C. Falco, M. Sevilla, Black perspectives for a green future: hydrothermal carbons for environment protection and energy storage, Energy & Environmental Science 5 (2012) 6796–6822.
[25] A. Tremel, J. Stemann, M. Herrmann, B. Erlach, H. Spliethoff, Entrained flow gasification of biocoal from hydrothermal carbonization, Fuel 102 (2012) 396–403.
[26] M.V. Gil, D. Casal, C. Pevida, J.J. Pis, F. Rubiera, Thermal behaviour and kinetics of coal/biomass blends during co-combustion, Bioresource Technology 101 (2010) 5601–5608.
[27] D.R. McIlveen-Wright, Y. Huang, S. Rezvani, J.D. Mondol, D. Redpath, M. Anderson, N.J. Hewitt, B.C. Williams, A techno-economic assessment of the reduction of carbon dioxide emissions through the use of biomass co-combustion, Fuel 90 (2011) 11–18.
[28] J. Li, A. Brzdekiewicz, W.H. Yang, W. Blasiak, Co-firing based on biomass torrefaction in a pulverized coal boiler with aim of 100% fuel switching, Applied Energy 99 (2012) 344–354.
[29] B.S. Hoffmann, A. Szklo, R. Schaeffer, An evaluation of the techno-economic potential of co-firing coal with woody biomass in thermal power plants in the south of Brazil, Biomass and Bioenergy 45 (2012) 295–302.
[30] M.L. Kubacki, A.B. Ross, J.M. Jones, A. Williams, Small-scale co-utilisation of coal and biomass, Fuel 101 (2012) 84–89.
[31] S.B. Lee, O. Fasina, TG–FTIR analysis of switchgrass pyrolysis, Journal of Analytical and Applied Pyrolysis 86 (2009) 39–43.
[32] G. Di Nola, W. de Jong, H. Spliethoff, TG–FTIR characterization of coal and biomass single fuels and blends under slow heating rate conditions: partitioning of the fuel-bound nitrogen, Fuel Processing Technology 91 (2010) 103–115.
[33] O. Fasina, B. Littlefield, TG–FTIR analysis of pecan shells thermal decomposition, Fuel Processing Technology 102 (2012) 61–66.
[34] M.X. Fang, D.K. Shen, Y.X. Li, C.J. Yu, Z.Y. Luo, K.F. Cen, Kinetic study on pyrolysis and combustion of wood under different oxygen concentrations by using TG–FTIR analysis, Journal of Analytical and Applied Pyrolysis 77 (2006) 22–27.
[35] A. Demirbas, Combustion characteristics of different biomass fuels, Progress in Energy and Combustion Science 30 (2004) 219–230.
[36] R. Bassilakis, R.M. Carangelo, M.A. Wojtowicz, TG–FTIR analysis of biomass pyrolysis, Fuel 80 (2001) 1765–1786.
[37] J. Shao, R. Yan, H. Chen, B. Wang, D.H. Lee, D.T. Liang, Pyrolysis characteristics and kinetics of sewage sludge by thermogravimetry Fourier transform infrared analysis, Energy & Fuels 22 (2008) 38–45.
[38] M.A. Lopez-Velazquez, V. Santes, J. Balmaseda, E. Torres-Garcia, Pyrolysis of orange waste: a thermo-kinetic study, Journal of Analytical and Applied Pyrolysis 99 (2013) 170–177.
[39] J. Cao, G. Xiao, X. Xu, D. Shen, B. Jin, Study on carbonization of lignin by TG–FTIR and high-temperature carbonization reactor, Fuel Processing Technology 106 (2013) 41–47.
[40] G.K. Parshetti, Z.G. Liu, A. Jain, M.P. Srinivasan, R. Balasubramanian, Hydrothermal carbonization of sewage sludge for energy production with coal, Fuel 111 (2013) 201–210.
[41] R.R. Baker, S. Coburn, C. Liu, J. Tetteh, Pyrolysis of saccharide tobacco ingredients: a TGA–FTIR investigation, Journal of Analytical and Applied Pyrolysis 74 (2005) 171–180.
[42] H.P. Yang, R. Yan, H.P. Chen, D.H. Lee, C.G. Zheng, Characteristics of hemicellulose, cellulose and lignin pyrolysis, Fuel 86 (2007) 1781–1788.
[43] J. Giuntoli, W. de Jong, S. Arvelakis, H. Spliethoff, A.H.M. Verkooijen, Quantitative and kinetic TG–FTIR study of biomass residue pyrolysis: dry distiller's grains with solubles (DDGS) and chicken manure, Journal of Analytical and Applied Pyrolysis 85 (2009) 301–312.
[44] W. de Jong, G. Di Nola, B.C.H. Venneker, H. Spliethoff, M.A. Wojtowicz, TG–FTIR pyrolysis of coal and secondary biomass fuels: determination of pyrolysis kinetic parameters for main species and NOx precursors, Fuel 86 (2007) 2367–2376.
[45] D.A. Dayton, Summary of NOx Emissions Reduction from Biomass Cofiring, DOE Contract DE - AC36 - 99 - GO10337, NREL/TP - 510–32260, National Renewable Energy Laboratory, Golden CO, May 2002. 3.
[46] D. Vamvuka, S. Troulinos, E. Kastanaki, The effect of mineral matter on the physical and chemical activation of low rank coal and biomass materials, Fuel 85 (2006) 1763–1771.
[47] F. Normann, K. Andersson, B. Leckner, F. Johnsson, High-temperature reduction of nitrogen oxides in oxy-fuel combustion, Fuel 87 (2008) 3579–3585.